

BASF NanoSelect™ Technology: Innovative Supported Pd- and Pt-based Catalysts for Selective Hydrogenation Reactions

Peter T. Witte · Peter H. Berben · Susan Boland ·
Evert H. Boymans · Dieter Vogt · John W. Geus ·
Johannes G. Donkervoort

Published online: 29 June 2012

© The Author(s) 2012. This article is published with open access at Springerlink.com

Abstract An innovative BASF catalyst manufacturing technology (NanoSelect™) is introduced which allows production of heterogeneous catalysts with excellent control over metal crystallite sizes. NanoSelect™ technology enabled the development of Pd catalysts which are lead-free Lindlar catalyst replacements in alkyne-to-*cis*-alkene hydrogenations. NanoSelect™ Pt catalysts showed excellent chemoselectivity in substituted nitro-arene hydrogenation reactions without build-up of hydroxylamine intermediates. All NanoSelect™ produced catalysts show markedly higher activity per gram of metal leading to ten-fold less use of precious metal.

Keywords NanoSelect™ · Catalyst · Catalysis · Lindlar replacement · Palladium · Platinum · Alkyne hydrogenation · Nitro group reduction

1 Introduction

Catalysts based on colloidal suspensions attracted much attention in recent years, both as supported [1] and as quasi-homogeneous [2] catalysts. These catalysts are

prepared by the so-called reduction-deposition method, where a metal is first reduced in solution in the presence of a stabilizer before it is deposited on a heterogeneous support. By using the appropriate reaction conditions, metal crystallites of <10 nm are available [3]. Catalysts produced in this way show sharper metal crystallite size distribution and do not contain large metal crystallites as sometimes observed in traditional catalysts (see right-hand side of Fig. 1).

For industrial applications the use of catalysts prepared by reduction-deposition is hampered by their cumbersome preparation. In general low metal concentrations are employed [4], but also the use of low-boiling organic solvents [5], high temperatures [6], very fast addition of reagents [7], or the use of reagents that are expensive or not commercially available [8] makes their production on an industrial scale difficult.

In this work, commercially available hexadecyl(2-hydroxyethyl)dimethyl ammonium dihydrogenphosphate (HHDMA, Fig. 2) is used as a water-soluble reagent for the preparation of metal nanoparticles. This reagent is combining both stabilizing and reducing functionalities in one molecule and in combination with its water solubility meets all requirements for use in commercial catalyst production. This innovative patent-protected [9] manufacturing technology, called NanoSelect™, has been used to prepare novel palladium and platinum based catalysts consisting of highly unimodal, colloidal metal particles supported on various support materials. With this technology, BASF was the recipient of the “2009 Frost & Sullivan North American Nanocatalysts Green Excellence of the Year Award”.

In this report we present the results leading to the development of palladium and platinum based catalyst and their use in specific organic reactions as highly selective

P. T. Witte · P. H. Berben · S. Boland · J. G. Donkervoort (✉)
BASF Nederland BV, Strijkviertel 67, 3454 PK De Meern,
The Netherlands
e-mail: hans.donkervoort@basf.com

E. H. Boymans · D. Vogt
Schuit Institute of Catalysis, Laboratory of Homogeneous
Catalysis, Eindhoven University of Technology, Eindhoven,
The Netherlands

J. W. Geus
Utrecht University, Padualaan 8, 3584 CH Utrecht,
The Netherlands

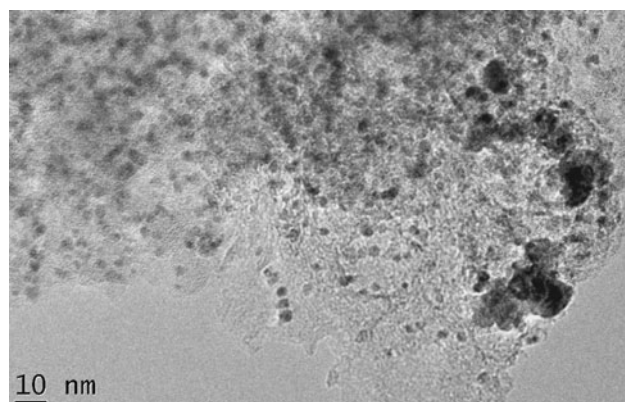


Fig. 1 TEM image of 5%Pd on C prepared by standard methods

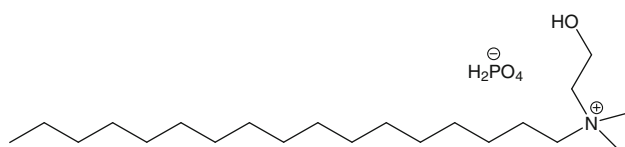


Fig. 2 Hexadecyl(2-hydroxyethyl)dimethyl ammonium dihydrogenphosphate

catalysts. Specifically, NanoSelect™ Pd catalysts were used in the selective hydrogenation of (substituted) alkynes to *cis*-alkenes and NanoSelect™ Pt catalysts for chemo-selective substituted nitro arene hydrogenation reactions.

2 Results and Discussion

2.1 Preparation of Colloidal Suspensions of Pd, Pt and Bimetallic Pd–Pt

Upon mixing HHDMA and Na_2PdCl_4 a colour change from yellow to red is observed. When a mixture of HHDMA and Na_2PdCl_4 is kept at room temperature, orange crystals form over a period of hours. A crystal structure determination [10] shows the hydrogen bonding of two units of the cationic moiety of HHDMA to a PdCl_4 anion (Fig. 3; Table 1). The alcohol functionality acts as a hydrogen bond donor, the metal-bound chlorine as acceptor. The Pd is located on an inversion center and the PdCl_4 moiety is therefore exactly planar.

At higher temperatures HHDMA is able to reduce Na_2PdCl_4 , which is indicated by a color change from red to

Fig. 3 Molecular structure of $(\text{HHDMA})_2\text{PdCl}_4$ in the crystal

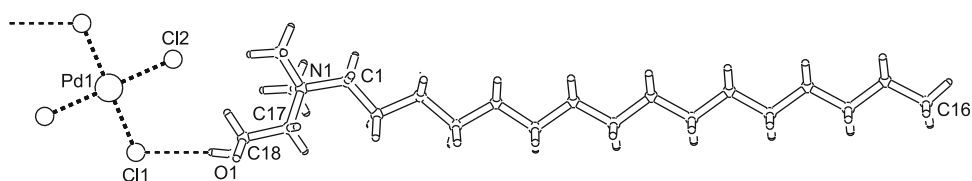


Table 1 Selected bond distances and angles in $(\text{HHDMA})_2\text{PdCl}_4$

Bond (Å)	Angle (°)	Hydrogen bond distance (Å)
Pd–Cl(1) 2.3069(4)	Cl(1)–Pd–Cl(2) 90.13(2)	Cl(1)···H(1o) 2.47(3)
Pd–Cl(2) 2.3017(4)	Cl(1)–Pd–Cl(2a) 89.87(2)	Cl(1)···O(1) 3.1988(16)

dark brown. Figure 4 shows a TEM image of a Pd colloidal suspension (from hereon referred to as c-Pd) formed in the presence of 10 eq. HHDMA. The metal crystallite size of the formed nanoparticles is 4–8 nm. When c-Pd is formed in the presence of 2 eq. HHDMA, TEM analysis shows that large agglomerates of Pd(0) particles are formed. Scanning transmission electron microscopy (STEM) measurements using a high angle annular dark field (HAADF) detector show that the agglomerates consist of Pd crystallites of the same size as those formed in the reaction with 10 eq. HHDMA. Apparently, 2 eq. HHDMA is sufficient for full reduction of Pd(II) to Pd(0), but not for stabilization of the formed Pd nanoparticles. Attempts to determine the oxidation product of HHDMA in the reaction mixture by ^{13}C NMR were unsuccessful because of the low concentration of the product.

The metal concentration used for the preparation of c-Pd (0.75 g/L Pd in H_2O) approaches the concentration used by Bönemann et al. (3.5 g/L Pd in THF) [11]. The concentration is more than 10 times higher than in the alcohol reduction method described by Toshima et al. (72 mg/L Pd in $\text{MeOH}/\text{H}_2\text{O}$) [5] and the citrate reduction method described by Turkevich et al. (33 mg/L Pd in H_2O) [4]. These last two methods use a stabilizer that is not chemically bound to the reductor. Turkevich states that doubling the metal concentration in his preparation leads to a significant increase of the Pd crystallite size. Using the same metal concentrations as for Pd and only a higher reduction temperature, we were able to prepare colloidal suspensions of Pt(0), and by mixing the Pd and Pt starting materials bimetallic colloidal particles could be prepared (metal crystallite size in c-Pt ~ 2 nm; c-PdPt 4–8 nm).

Agglomeration of metal crystallites is proposed to be prevented by the steric bulk of the C16 alkyl chain of the organic moiety of HHDMA [1–3]. This would explain the results obtained using choline ($\text{Me}_3\text{N}^+\text{CH}_2\text{CH}_2\text{OH}$) to reduce Na_2PdCl_4 . Although the normal color changes are

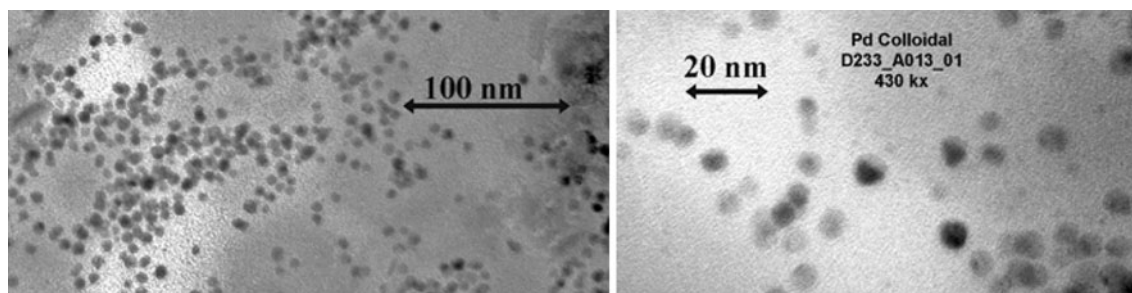


Fig. 4 TEM image of c-Pd formed with 10 eq. HHDMA

observed upon addition and heating to 80 °C (yellow to red to dark brown), a black precipitate is formed within minutes at 80 °C. The much smaller organic moiety of choline seems not to have the ability to stabilize Pd crystallites at this temperature, leading to agglomeration and finally precipitation of Pd-black.

The traditional way of describing a metal particle in a colloidal suspension, is through the polar ammonium functionality directed towards the metal center and the a-polar alkyl chain sticking out. This is corroborated by results obtained in XANES studies on colloidal metal suspensions in organic solvents which indicate reduced metal surfaces to interact with the ionic moiety of alkyl ammonium stabilizers [12]. However, this description would not explain why the metal particles formed with HHDMA are highly soluble in water and cannot be extracted into an organic solvent. It is therefore proposed that the metal particles formed in the NanoSelect™ protocol are stabilized by a double layer of HHDMA, where the outer shell of the colloidal particle exists of ammonium functionalities of the second HHDMA layer. Alternatively, an inverted monolayer with the polar functionalities sticking out into the aqueous solution and the a-polar alkyl chains interacting with the metal surface could be envisioned.

2.2 Deposition of metal nanoparticles on a heterogeneous support

Mixing c-Pd, c-Pt or c-PdPt with a heterogeneous support, like activated carbon (C) or titanium silicate (TiS), yields the supported metal particles (Fig. 5).

TEM imaging shows that at high metal loadings (~1 %) the metal crystallites cluster to form large agglomerates. In these agglomerates not all colloidal particles are directly bound to the support and unsupported particles are often observed, probably formed during the ultrasonic pre-treatment of the TEM samples. This is never observed in TEM pictures of catalysts of low metal loadings, in which all colloidal particles are directly bound to the support. Apparently the colloid-support interaction is stronger than the colloid–colloid interaction. When free HHDMA is added to

the support before metal deposition, the maximum metal loading is drastically decreased. This shows that HHDMA competes with c-Pd for active sites on the support, so it is likely that both bind through the same mechanism.

The bimetallic c-PdPt/TiS was analyzed by STEM–energy dispersive X-ray analysis (EDX). The very high resolution of this analysis is unique (an electron beam with a diameter of 0.8 nm is used) and allows for the elemental analysis of individual metal crystallites. A scan over the surface of the material showed that all peaks of Pt and Pd coincide, so the metal crystallites are truly bimetallic (Fig. 6). No monometallic metal crystallites, indicated by a peak of only Pt or only Pd, were observed.

The IR spectrum of TiS support shows peaks at 3,700 cm^{-1} from Ti- and Si–OH groups and at 1,640 cm^{-1} from absorbed water. The water peak is also observed in the spectrum of c-Pd/TiS, but here the peak at 3,700 cm^{-1} is not found. The Ti- and Si–OH groups are clearly involved in the bonding of the Pd colloids, probably by exchange with phosphate anions. IR spectroscopy shows that water is removed after heating c-Pd/TiS to 350 °C (HHDMA remains bound to the catalyst), while heating a TiS sample to 250 °C is sufficient to remove all water. This indicates that water is more strongly bound to c-Pd/TiS than to TiS, probably because of interaction with the hydrophilic HHDMA. This is consistent with TGA measurements that show that all water is removed from TiS at 250 °C, while c-Pd/TiS needs to be heated to 400 °C to remove all water.

2.3 Semi-Hydrogenation of 3-Hexyn-1-ol by c-Pd/TiS

Several catalysts were tested in the hydrogenation of 3-hexyn-1-ol using the same amount of supported catalyst, although the metal loading differed significantly (Scheme 1). Full hydrogenation to hexanol is achieved by 2.0 L of H_2 . When a Pd/C catalyst prepared by standard methods is used, a fast uptake of 2.1 L of H_2 is observed (Fig. 7a). GC analysis shows full conversion to hexanol and the additional formation of hexane by C–O hydrogenolysis, which explains why the H_2 uptake stops only after 2.1 L H_2 . When this Pd/C is treated with HHDMA, the H_2

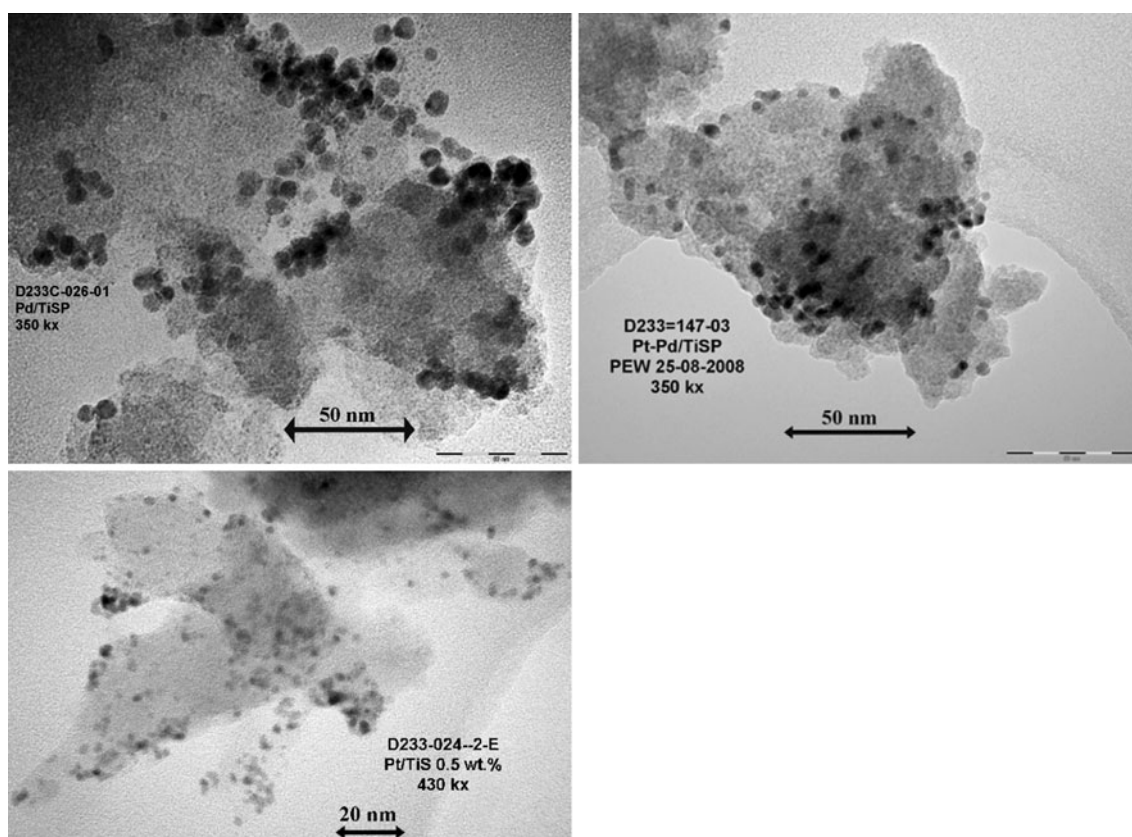


Fig. 5 TEM images: *top left*) c-Pd/TiS; *top right*) c-PdPt/TiS *bottom*) c-Pt/TiS

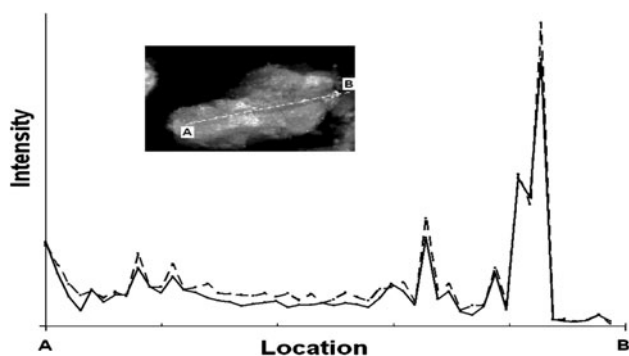


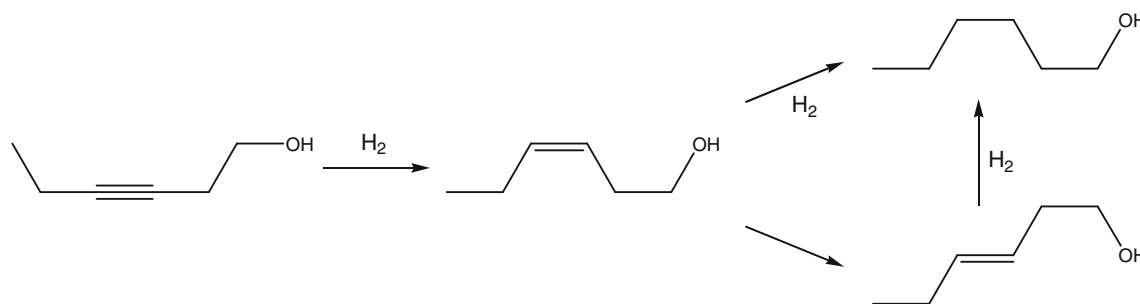
Fig. 6 STEM-EDX analysis of c-PdPt/TiS; Pt (*dashed lines*); Pd (*continuous lines*); distance A–B 110 nm

uptake curve shows that the catalyst activity is lower in the second part of the reaction, although this reaction is still taking place at a considerable rate. The H_2 uptake stops after 2.0 L, and GC measurements show only formation of hexanol. Clearly, addition of HHDMA to Pd/C, makes this catalyst somewhat more selective.

The H_2 uptake curve of c-Pd/TiS shows a slower H_2 uptake, which stops after 1.0 L H_2 is consumed (Fig. 7c), indicating a selective semi-hydrogenation to the olefin. When the reaction is stopped immediately after the consumption of 1.0 L H_2 , GC analysis shows a high selectivity

towards the *cis*-olefin. Since the unsupported c-Pd also turned out to be active and selective in this test reaction, hot filtration experiments were performed to see if the hydrogenation was quasi-homogeneous or purely heterogeneous. It was found that Pd leaching takes place at high metal loading, which is consistent with the weak bonding of metal agglomerates mentioned above.

The catalyst most often used for the semi-hydrogenation of substituted alkynes is Lindlar catalyst (5%Pd + 2–3%Pb on $CaCO_3$). Because of environmental reasons the use of Pb is not desirable. When Lindlar catalyst is used in our test reaction, the H_2 uptake curve shows that this hydrogenation also stops after 1.0 L H_2 is consumed (Fig. 7d). However, the exact end point of the reaction is more difficult to determine, since the reaction slows down significantly before full conversion is reached. Although the H_2 consumption does not exceed 1.0 L, prolonged reaction times should be avoided since this leads to *cis*–*trans* isomerization. GC analysis shows that the Lindlar catalyst has a high *cis*-selectivity (>99 % after 40 min reaction time) at 95 % conversion, while this has lowered to 97 % at full conversion (100 min reaction time). When the hydrogenation using c-Pd/TiS is continued after uptake of 1.0 L H_2 , very slow overhydrogenation, *cis*–*trans* isomerisation and isomerisation to 2- and 4-hexenol is observed (Table 2).

Semi-hydrogenation of 3-hexyn-1-ol by *c*-Pd/TiS

Scheme 1 Hydrogenation of 3-hexyn-1-ol to the *cis*-3-hexen-1-ol and formation of byproducts

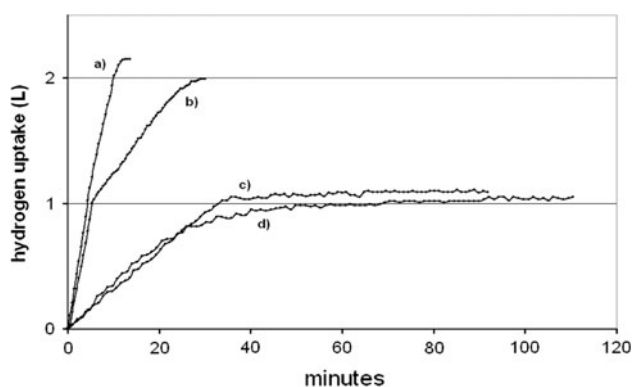


Fig. 7 H₂ uptake curves for 3-hexyn-1-ol hydrogenation: **a** Pd/C, **b** Pd/C treated with HHDMA, **c** *c*-Pd/TiS, **d** Lindlar

Table 2 Catalytic hydrogenation of alkynes: R¹-C≡C-R² → R¹-CH=CH-R²

R ¹	R ²	Catalyst	Conversion (%)	Olefin (%)	Cis-olefin (%)
CH ₂ CH ₃	CH ₂ CH ₂ OH	<i>c</i> -Pd/TiS	97	99	97
CH ₂ CH ₃	CH ₂ CH ₂ OH	Lindlar	>99	99	97
H	CMe ₂ OH	<i>c</i> -Pd/TiS	97	95	n.a.
H	CMe ₂ OH	Lindlar	>99	96	n.a.
H	Ph	<i>c</i> -Pd/TiS	93	94	n.a.
H	Ph	Lindlar ^a	95	97	n.a.
Me	Ph	<i>c</i> -Pd/TiS ^a	90	89	97
Me	Ph	Lindlar ^a	48 ^b	96	98

^a Five times more catalyst used

^b Reaction stops before full conversion is reached

2.4 Chemoselective Hydrogenation of Nitro Arenes Using Pt Catalysts

The supported *c*-Pt catalysts were tested in the chemoselective hydrogenation of nitro arenes. The chemo-selective full hydrogenation of the nitro arene leads to 1.5 L H₂ consumption. Typical hydrogen uptake curves are shown in Fig. 8.

The unpromoted *c*-Pt/C show initial fast hydrogen uptake but after approximately 60 % conversion the reaction rate slows down with concomitant build up of significant amounts of the intermediate hydroxylamine as shown by GC analysis. When molybdenum is used as promoter to the catalyst, the initial reaction rate is retained also at high conversion levels and no hydroxylamine build up was observed. The molybdenum is believed to catalyze the disproportionation of the hydroxylamine thereby maintaining the fast initial reaction rate. Due to this effect, the build up in the reactor of hydroxylamine is minimized making this process much safer on large scale.

In Table 3, results are presented for the hydrogenation of 2-chloronitrobenzene with various platinum catalysts tested at the same metal loading in the reactor. For all catalysts no azo- or azoxy-species are observed in the final product under the reaction conditions applied. Both promoted and un-promoted catalysts show high selectivity towards the 2-chloroaniline with only minimal dhalogenation taking place. When the catalyst amount is decreased by 50 %, selectivity increases from 96 to 98 % while time to full conversion increases from 60 to 120 min

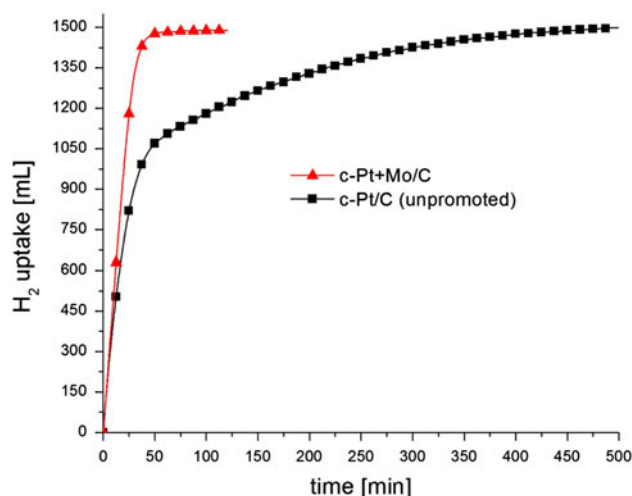


Fig. 8 Typical hydrogen uptake curves for nitro arene hydrogenation

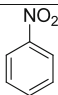
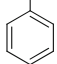
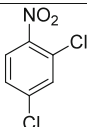
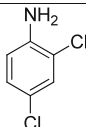
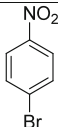
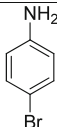
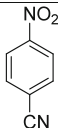
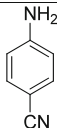
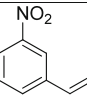
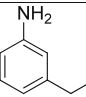
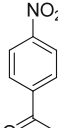
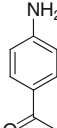
Table 3 Hydrogenation of 2-chloronitrobenzene with Pt catalysts

Entry	Catalyst	Selectivity (%)	Time to full conversion (min)
1	c-Pt/C	99	500
2	c-Pt + Mo/C	96	60
3	c-Pt + Mo/C ^a	98	120
4	(1%Pt + 2%V)/C	98	200

^a Half the amount of catalyst used

(Table 3, entry 2 and 3). This indicates that optimizing reaction conditions for the specific substrate of choice can lead to further improvements in the process outcome. To

Table 4 Hydrogenation of substituted nitro-arene compounds with c-Pt(Mo)/C

entry	Substrate	Product	Selectivity	Time to full conversion [min]
1			>99	50
2			98	70
3			93	50
4			99	400
5			99	1000
6			93	170

compare NanoSelectTM catalysts with commercially available catalysts specifically developed for this type of chemoselective transformation, the vanadium promoted Pt catalyst developed by Baumeister et al. [13]. was tested in the same process. As can be seen in Table 3 (entry 4), this catalyst is performing the chemoselective nitro arene hydrogenation giving similar selectivities. However, the observed activity of this catalyst is substantially lower, leading to longer reaction times or the use of larger amounts of platinum compared to the c-Pt catalysts. Other substrates were tested to investigate the chemoselectivity of the Mo-promoted c-Pt/C. These results are reported in Table 4.

As can be clearly seen from the results reported in Table 4, the c-Pt catalysts are excellent catalysts for the chemoselective hydrogenation of various substituted nitro arene compounds. Not only mono-chloro but also di-chloro (entry 3) and mono-bromo substituted nitro-arenes are reduced with high retention of the other substituent. In addition, nitrile and carbonyl groups are retained with excellent selectivity. So far, it has not been possible to perform the selective hydrogenation of nitro styrene (entry 5) under the conditions described. However, recent preliminary results indicate also this chemoselective hydrogenation can be achieved successfully by using the right c-Pt catalyst and modified reaction conditions. These results will be reported in the near future.

3 Conclusions

BASF developed an innovative method for preparing mono- and bimetallic precious metal catalysts through reduction-deposition that is suitable for large-scale production which is called NanoSelectTM. Using NanoSelectTM technology, innovative Pd-catalysts were produced which show high activity and selectivity in the semi-hydrogenation of substituted alkynes to the corresponding *cis*-alkenes. As such these catalysts are replacements of the classical Lindlar catalyst with the huge environmental advantage that no lead is needed to accomplish same levels of activity and selectivity.

Also NanoSelectTM Pt catalysts for the chemoselective hydrogenation of nitro arenes were developed. These catalysts show high hydrogenation activity towards the respective amine with good to excellent chemoselectivity. For example, chemoselective nitro arene hydrogenation can be accomplished in the presence of halides, nitriles, or carbonyl functionalities. In addition, NanoSelectTM technology enabled modifications of these Pt-based catalysts which resulted in minimizing the buildup in the reactor of the potentially explosive hydroxylamine intermediate. This makes the process safer to handle on small and large scale.

4 Experimental Section

4.1 Preparation of Catalysts [9]

c-Pd A solution of 15 g HHDMA in 1 L water was heated to 60 °C. A solution of 0.75 g Pd (as Na₂PdCl₄) in 10 mL water was added. The mixture was heated to 80 °C and stirred at this temperature for 2 h. *c-Pt*: As Pd, but using H₂PtCl₆ and a reaction temperature of 95 °C. *c-PdPt*: As Pt, but using a mixture of equal amounts of Pd and Pt. *c-Pd/TiS*: A slurry of 75 g TiS powder in 750 mL water was stirred for 30 min at room temperature, after which *c-Pd* was added. After an additional 45 min of stirring, the catalyst was filtered off and washed. Analysis: 0.47 % Pd, 6.1 % C, 18 % water. IR (cm⁻¹): 1200 (TiS support), 1640 (water), 1410, 1470, 2855, 2925 + shoulder (HHDMA). TGA (weight loss): 6 % 25–100 °C, 4 % 100–300 °C, 6 % 300–400 °C, 0 % 400–650 °C. PSD: d(0.1) 5.0 d(0.5) 22.4 d(0.9) 47.8. *c-Pd/C*: As *c-Pd/TiS*, but using carbon powder. Analysis: 0.60 % Pd, 63 % water.

4.2 Hydrogenation of 3-Hexyn-1-ol [9]

Pd/C, *c-Pd/TiS*: A 250 mL stainless steel autoclave was charged with 50 mg catalyst (dry weight), 100 mL 96 % ethanol, and 5 mL 3-hexyn-1-ol and the mixture was heated to 30 °C. Without stirring, the autoclave was flushed with hydrogen and pressurized with 3 bars of hydrogen. The reaction was started by starting the stirring (1500 rpm). Lindlar: As *Pd/C* and *c-Pd/TiS*, but with a 15 min prehydrogenation step.

4.3 Hydrogenation of Nitro Arenes

A 100 mL stainless steel autoclave was charged with 27.3 mg catalyst (dry weight), 22.3 mmol substrate ($S/C = 20 \times 10^3$) and 80 mL absolute ethanol and the mixture was heated to 30 °C. Without stirring, the autoclave

was flushed with hydrogen and pressurized with 3 bars of hydrogen. The reaction was started by starting the stirring (1,500 rpm). Samples were analyzed by GC (PONA column), where the selectivities were determined as area % in summarized products.

Acknowledgments We gratefully acknowledge Dr Guido Mul and Ana Rita Almeida of TU Delft for their help with IR and TGA measurements.

Open Access This article is distributed under the terms of the Creative Commons Attribution License which permits any use, distribution, and reproduction in any medium, provided the original author(s) and the source are credited.

References

1. Roucoux A, Schulz J, Patin H (2002) Chem Rev 102:3757
2. Astruc D, Lu F, Aranzas JR (2005) Angew Chem Int Ed 44:7852
3. Bönemann H, Nagabhushana KS (2007) Metal nanoclusters in catalysis and materials science. In: Corain B, Schmid G, Toshima N (eds) The issue of size control, Part 1, Chapt. 2. Elsevier, Amsterdam, and references therein
4. Turkevich J, Kim G (1970) Science 169:873
5. Hirai H, Chawanya H, Toshima N (1985) React Polym 3:127
6. Bonet F, Delmas V, Grugeon S, Herrera Urbina R, Silvert P-Y, Tekaiia-Elhissen K (1999) Nanostruc Mat 11:1277
7. Lu W, Wang B, Wang K, Wang X, Hou JG (2003) Langmuir 19:5887
8. Bönemann H, Brijoux W, Brinkmann R, Dinjus E, Jousen T, Korall B (1991) Angew Chem Int Ed 30:1312
9. Witte, PT (2009) WO patent (2009) 096783
10. CCDC 754963 contains the supplementary crystallographic data for this paper. These data can be obtained free of charge from The Cambridge Crystallographic Data Centre via www.ccdc.cam.ac.uk/data_request/cif
11. Bönemann H, Brinkmann R (1994) Appl Organometal Chem 8:361
12. Bucher S, Hormes J, Modrow H, Brinkmann R, Waldöfner N, Bönemann H, Beuermann L, Krischok S, Maus-Friedrichs W, Kemper V (2002) Sur Sci 497:321
13. Baumeister P, Blaser H-U, Studer M (1997) Catal Lett 49:219